

Temperature-dependent photoabsorption cross-sections of cyanoacetylene and diacetylene in the mid- and vacuum-UV: Application to Titan's atmosphere

T. Ferradaz^{a,*}, Y. Bénilan^a, N. Fray^a, A. Jolly^a, M. Schwell^a, M.C. Gazeau^a, H.-W. Jochims^b

^aLISA, Laboratoire Interuniversitaire des Systèmes Atmosphériques, UMR 7583, Universités Paris 7 et Paris 12, 61 avenue du Général de Gaulle, 94010 Créteil Cedex, France

^bInstitut für Physikalische und Theoretische Chemie der Freien Universität Berlin, Takustr. 3, 14195 Berlin, Germany

Received 11 July 2008; received in revised form 8 October 2008; accepted 8 October 2008

Available online 25 October 2008

Abstract

Cyanoacetylene (HC₃N) and diacetylene (C₄H₂) play an important role in the photochemistry of Titan's atmosphere, in part because of their strong absorption between 110 and 180 nm. Accurate photoabsorption cross-sections at temperatures representative of Titan's atmosphere are required to interpret Cassini observations and to calculate photolysis rates used in photochemical models. Using synchrotron radiation as a tunable vacuum ultraviolet (VUV) light source, we have measured absolute photoabsorption cross-sections of C₄H₂ and HC₃N with a spectral resolution of 0.05 nm in the region between 80 and 225 nm and at different temperatures between 173 and 295 K. The measured cross-sections are used to model transmission spectra of Titan atmosphere in the VUV.

© 2008 Elsevier Ltd. All rights reserved.

Keywords: Cyanoacetylene; Diacetylene; Absorption cross-sections; Vacuum ultraviolet; Low temperatures; Titan

1. Introduction

Titan, the largest satellite of Saturn, is the only body in the Solar System besides the Earth with a dense atmosphere mainly composed of dinitrogen (N₂). It also contains a large amount of methane (CH₄), around 5% in the troposphere and 1.5% in the stratosphere (Niemann et al., 2005; Flasar et al., 2005). High-energy electrons from Saturn's magnetosphere and solar UV photons induce the dissociation of N₂ and CH₄ in the upper atmosphere. The recombination of the fragments initiates an organic chemistry that leads to the production of numerous saturated and unsaturated hydrocarbons and nitriles. Many of those molecules have been detected from the analysis of ultraviolet and infrared spectra recorded by the Voyager missions (Hanel et al., 1981; Kunde et al., 1981;

Smith et al., 1981) and confirmed by ISO observations (Coustenis et al., 2003). Some more complex and heavier molecules up to C₆ have been revealed in situ in Titan's upper atmosphere by the Cassini ion and neutral mass spectrometer (INMS) (Waite et al., 2005). Recent spectroscopic observations by the composite infrared spectrometer (CIRS) (Teauby et al., 2007; Coustenis et al., 2007) and the ultraviolet imaging spectrograph (UVIS) (Shemansky et al., 2005) onboard the Cassini spacecraft have confirmed the chemical diversity of Titan's atmosphere.

Two of the minor and heaviest constituents detected in Titan's atmosphere are cyanoacetylene (HC₃N) and diacetylene (C₄H₂) (also called propynenitrile and butadiyne). They have been identified for the first time by Voyager infrared measurements (Kunde et al., 1981). The stratospheric abundance of both compounds shows a significant increase from southern to northern latitudes (Coustenis et al., 2007; Coustenis and Bézard, 1995).

HC₃N is a member of the cyanopolyynes series with the general formula H-(C≡C)_n-C≡N, $n > 1$, while C₄H₂ ($n = 2$) is the first member of the polyynes with the general

*Corresponding author. Tel.: +33 01 45 17 15 38; fax: +33 01 45 17 15 64.

E-mail addresses: ferradaz@lisa.univ-paris12.fr (T. Ferradaz), benilan@lisa.univ-paris12.fr (Y. Bénilan).

formula $\text{H}-(\text{C}\equiv\text{C})_n-\text{H}$. Cyanopolyynes are easily observable in the interstellar medium (ISM) by microwave observations because they have a strong permanent dipole moment. HC_3N has been detected for the first time in the ISM by microwave spectroscopy (Turner, 1971). Since then, longer chains, up to HC_{11}N , have been observed too (Bell et al., 1997). On the contrary, polyynes have no permanent dipole moment and are much more difficult to observe. C_4H_2 and C_6H_2 are the only polyynes observed so far. They have been identified in the infrared range in the circumstellar envelope of CRL618 by ISO (Cernicharo et al., 2001). The study of polyynes and cyanopolyynes are of special interest for Titan since they are predicted by photochemical models to be possible haze precursors (Yung et al., 1984; Lavvas et al., 2008). Thick layers of haze are observed in Titan's atmosphere and are responsible for the satellite's orange color. HC_3N is also important from an exobiological point of view since it is an intermediate in a prebiotic synthesis of cytosine proposed by Orgel (2002).

Complementary to infrared and microwave spectroscopy, UV spectroscopy is also a powerful diagnostic tool in the study of organic composition and chemical process in planetary atmospheres. Vacuum ultraviolet (VUV) spectroscopy sounds the upper atmosphere, from the thermosphere down to the upper stratosphere. The UVIS instrument on board the Cassini spacecraft is able to acquire spectra in Titan's atmosphere in the Far UV range (110–190 nm) with a resolution of 0.275 nm (Esposito et al., 2004). During Titan flyby labeled T_B , stellar occultation absorption spectra have shown the presence of several species including C_4H_2 (Shemansky et al., 2005).

The interpretation of spectra in the VUV range is critically dependent on the knowledge of the absorption coefficients of the molecules in the same temperature conditions as in the planetary environment (Jolly and Bénilan, 2008). Cross-sections in this wavelength range are also needed to calculate photolysis rates which are essential parameters for photochemical models. Unfortunately, for many organic compounds of planetological interest, ultraviolet spectra are not well known or even unavailable, especially at low temperatures.

The absolute absorption coefficient of HC_3N between 105 and 165 nm has already been measured by Connors et al. (1974) at room temperature. In the mid-UV domain (185–230 nm), temperature dependent studies have been carried out before (Bénilan et al., 1994; Andrieux et al., 1995) and it is interesting to note that significant differences have been observed (Bénilan et al., 1996).

The VUV spectrum of C_4H_2 has been obtained by Kloster-Jensen et al. (1974) at room temperature, in the wavelength range 122–276 nm, but only the relative intensities have been measured in this work. Absolute cross-sections values at room temperature have been obtained by Okabe (1981) and Glicker and Okabe (1987), in the 120–260 nm region. The temperature dependence of the ultraviolet absorption cross-sections has also been

measured, but only between 160 and 220 nm with a resolution of 0.1 nm for temperatures ranging from about 220–330 K (Fahr and Nayak, 1994). In another study in the mid-UV range (195–265 nm), at 0.02 nm resolution, absolute absorption cross-sections were determined at various temperature between 193 and 293 K (Smith et al., 1998). Both studies have demonstrated significant effects of the temperature on cross-sections, in particular variation of band intensities.

It appears that for both molecules, temperature dependent studies are lacking below 160 nm where both molecules have their strongest absorption. Therefore, we have measured the temperature dependent absorption cross-sections of HC_3N and C_4H_2 in the gas phase between 80 and 225 nm at various temperatures between 170 and 298 K.

In Section 2, we present the experimental setup and the data reduction procedure used to determine cross-sections from synchrotron radiation absorption. In the Section 3, we show the results and discuss the effects of temperature on the absorption coefficients. Finally, we discuss in Section 4 the influence of our new laboratory measurements on the interpretation of Titan's atmospheric ultraviolet spectra.

2. Experimental method and procedures

C_4H_2 was prepared by dehydrochlorination of 1,4-dichloro-2-butyne ($\text{C}_4\text{H}_4\text{Cl}_2$) (Khelifi et al., 1995) in tetraethylene diethyl ether to which 40% aqueous sodium hydroxide solution was slowly added. Once formed, the compound was carried away in a stream of nitrogen, dried over calcium chloride and was trapped with an acetone/liquid nitrogen slush (–25 to –30 °C). It has then been distilled at –70 °C in order to eliminate impurities. This process was monitored using infrared spectroscopy.

HC_3N was synthesized according to the method of Moureu and Bongrand (1920) modified later by Miller and Lemmon (1967). In this procedure, ammonia is added on methylpropiolate and the corresponding amide is dehydrated to yield HC_3N . The purity of the final product was also checked by infrared spectroscopy. Both compounds were stored at liquid nitrogen temperature to avoid any polymerization.

Tunable VUV light was obtained from the synchrotron radiation facility BESSY in Berlin. A first set of measurements was made in the 80–200 nm spectral region at 0.3 nm resolution with the 10 m focal length normal incidence monochromator (NIM) at the U125/2 undulator beamline. A linear dispersion of 0.08 nm mm^{-1} was reached by using the first order of a 1200 lines/mm spherical grating. The recorded data were self-calibrated in wavelength by a stepwise system inside the monochromator (Reichardt et al., 2001a). To allow for measurements below windows cutoffs, the window (cf. Fig. 1) was replaced by a micro channel plate (MCP) and a differential pumping system. An MCP allows for VUV light transmission and at the same

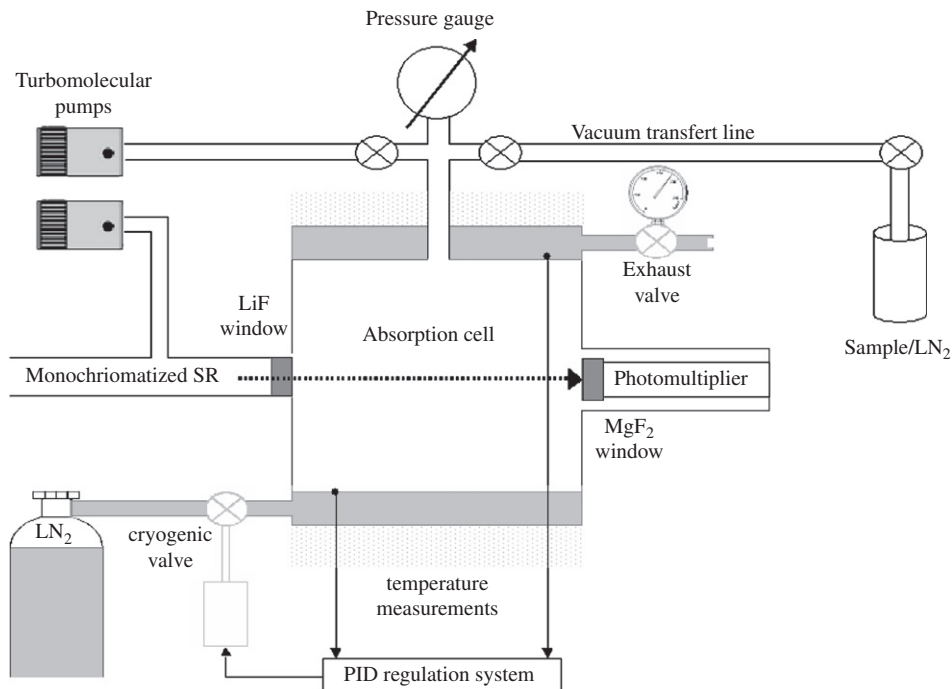


Fig. 1. Experimental setup used for measuring the ultraviolet absorption spectra at low temperatures.

time, a pressure gap of three orders of magnitude is realized, permitting application of the Beer–Lambert Law. Light detection was performed by a photomultiplier tube sensitive to visible light produced by fluorescence of sodium salicylate deposited on the exit BK7 glass window when excited by VUV photons. All results presented in this paper for the 80–115 nm range have been obtained with this configuration.

A second set of measurements have been taken between 115 and 225 nm using a 3 m focal length NIM equipped with a 600 lines/mm holographically ruled grating giving a linear dispersion of 0.56 nm mm^{-1} , connected to a dipole magnet beamline (DIP 12-1B) (Reichardt et al., 2001b). In these experiments, we reached an instrumental bandwidth (FWHM) of 0.05 nm. Wavelength calibration was obtained by using the first self-calibrated set of measurements as a reference. The VUV radiation intensity was measured directly with a solar blind photomultiplier tube closed by a MgF_2 window (Electron Tubes Limited 9402B with caesium telluride photocathode). The absorption cell is a cylinder (volume = 940 cm^3) with an optical pathlength of 11.77 cm (Fig. 1). In the second set of measurements, a LiF window was placed at the entrance of the cell instead of the MCP as presented in Fig. 1. The use of an holographically ruled grating with aluminum/ MgF_2 coating provides low diffused light and the LiF window suppresses second order emission. Low temperatures in the cell were obtained by flowing liquid nitrogen in the double wall surrounding the cell. During the experiments, the temperature is measured continuously at two diametrically opposite positions with Type-K thermocouples fixed on the inside wall of the cell. The cell temperature is regulated by controlling the flow of liquid nitrogen through a cryogenic valve, making use of a

standard proportional, integral, and derivative (PID) controller. The stability of the temperature is $\pm 1 \text{ K}$ over a period of 8 h and thermal equilibrium is usually obtained after 1 h with a measured temperature gradient of $< 2 \text{ K}$ over the absorption path. The cooling system allows us to reach almost liquid nitrogen temperatures but no experiment have been done below 170 K, since at such a temperature, the vapour pressure of the studied molecules drops below $1 \mu\text{bar}$ which is close to the current limit of our pressure measurement system.

The signal was recorded through a picoammeter (Keithley) using an integration time of 1 s per sample. Absolute photoabsorption cross-sections are calculated using the Beer–Lambert law:

$$\sigma = (1/l) \times \ln(I_0/I) \times (1013/P) \times (T/273) \quad (1)$$

σ corresponds to the absolute absorption coefficient (in $\text{cm}^{-1} \text{ amagat}^{-1}$), I_0 is the light intensity transmitted with an empty cell, I is the light intensity transmitted through the gas sample, l the absorption path length (cm) and T (K) and P (mbar) are respectively the temperature and the pressure of the sample. Since the intensity of the light flux decreases with time, due to the decay of the storage ring current, I_0 is estimated by an interpolation between empty cell scans recorded before and after the spectra.

In the second data set, the use of an MgF_2 window to protect the solar blind photomultiplier prevents measurement of any flux below about 113 nm due to the transparency cut-off. Note that, similarly to previous studies (Hunter and Malo, 1969), we observe a shift of the short-wavelength cut-off as the temperature decreases (Fig. 4).

For each recorded spectrum, the sample is vaporized into the cell at the desired pressure which is monitored with an MKS baratron capacitance manometer (10^{-4} to 1 mbar). In the VUV domain, all measurements were made at pressures between 3 and 20 μ bars to avoid any saturation of absorption features. In the mid-UV range, pressures of up to 100 μ bars were used. For a given spectral region, at least four different pressures are used to check the reproducibility of the measurements and to make sure that the data are free from saturation. We verified that the data follow the Beer–Lambert law over the studied pressure range.

Experimental uncertainties on the cross-section determinations are estimated to be about 10%. This is mainly due to pressure measurements uncertainties and errors in the determination of the I_0 continuum level. In the mid-UV domain, uncertainties may reach 20% because of incident light fluctuations caused by the weakness of the synchrotron radiation above 200 nm. The consequence is a larger error on the determination of the I_0 continuum value. Also, a small path length is not well adapted in this spectral domain where small absorption coefficients are observed and hence large pressures are needed. In fact, the molecules' saturation vapour pressure values at low temperature are in fact limiting our ability to work at higher pressures.

3. Results and discussion

3.1. Cyanoacetylene

3.1.1. Photoabsorption by HC_3N at room temperature

Fig. 2 shows the absolute photoabsorption coefficient of HC_3N in the spectral region from 80 to 220 nm determined at room temperature (298 K). The experimental resolution

is 0.3 nm below 115 and 0.05 nm from 115 to 225 nm. For the sake of completeness, we also show absorption cross-sections.

The absorption spectra of HC_3N exhibits a complex vibrational structure from 180 to 230 nm assigned to the forbidden electronic transition $^1\Delta_u \leftarrow ^1\Sigma_g^+$ (Job and King, 1966; Bruston et al., 1989). The vibronic bands arise from the Herzberg–Teller effect: the intensity is borrowed from the allowed transitions by π -type vibrations. In this wavelength domain, the absolute absorption coefficient and its temperature dependency has already been studied by Bénilan et al. (1994).

Between 105 and 165 nm, Connors et al. (1974) room temperature study is the only one that reports absolute absorption cross-section measurements. The first transition extending from 151–164 nm has been assigned to a $^1\Pi_u \leftarrow ^1\Sigma_g^+$ transition by these authors. This system shows two doublets separated by about 2060 cm^{-1} , which implies the active $\nu_3^+(\sigma^+)$ vibration mode measured at 2079 cm^{-1} in the $^1\Sigma_g^+$ electronic ground state (Jolly et al., 2007). A strong and diffuse intravalence shell band is observed with an origin at 145 nm. It has been assigned to a $^1\Sigma_u^+ \leftarrow ^1\Sigma_g^+$ transition by Connors et al. (1974). A second peak is present at 141 nm separated by 1910 cm^{-1} from the previous one corresponding most likely again to excitation of the $\nu_3^+(\sigma^+)$ vibration. This diffuse system is followed by several strong and sharp transitions which have been assigned by Connors et al. (1974) to Rydberg series converging to the first ionization energy at 11.6 eV (106.9 nm). As seen in Fig. 2, the absorption coefficient varies by 3 orders of magnitude in the entire UV region, with a maximum of 6125 $\text{cm}^{-1}\text{.am}^{-1}$ at 145 nm.

Our cross-section values below 165 nm are in very good agreement with those of Connors et al. (1974) for the larger

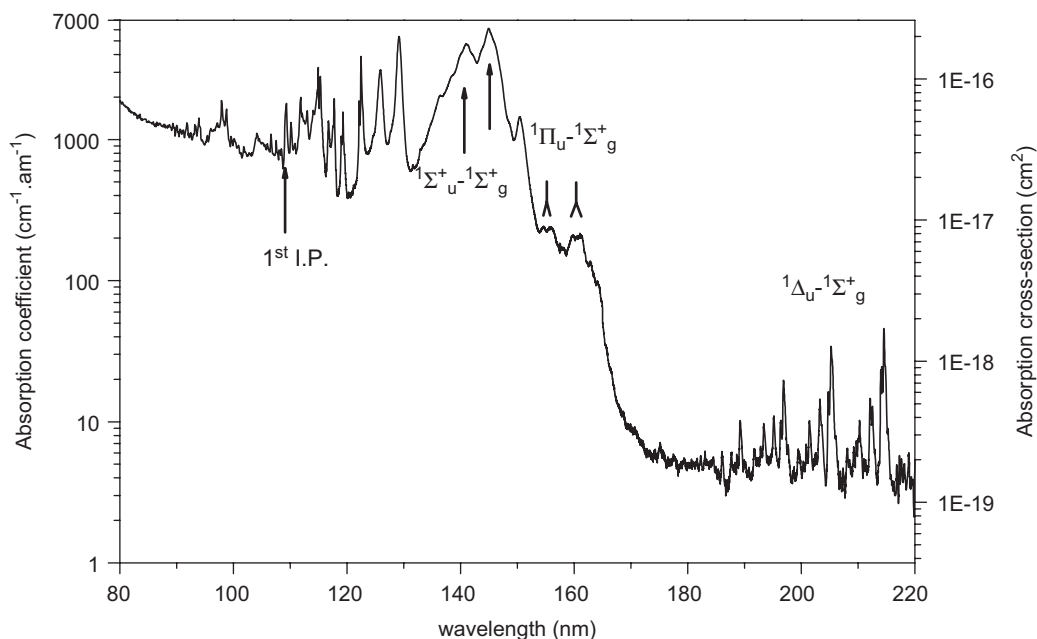


Fig. 2. Absolute photoabsorption cross-section of HC_3N between 80 and 225 nm at room temperature. The main electronic transitions are shown.

Table 1
Absorption cross-sections (in $\text{cm}^{-1} \text{am}^{-1}$) for selected peaks of HC_3N measured in this work and in previous work and the percentage changes $P_{c,203\text{K}}$ and $P_{c,243\text{K}}$.

λ (nm)	Connors et al. (1974) ($\text{cm}^{-1} \text{am}^{-1}$)	$\sigma_{298\text{K}}$ ($\text{cm}^{-1} \text{am}^{-1}$)	$\sigma_{243\text{K}}$ ($\text{cm}^{-1} \text{am}^{-1}$)	$\sigma_{203\text{K}}$ ($\text{cm}^{-1} \text{am}^{-1}$)	$P_{c, 243\text{K}}$	$P_{c, 203\text{K}}$
114.5		1584	1559	1599	−1.6	0.9
114.8		2192	2176	2233	−0.7	1.9
114.9		3235	3373	3553	4.3	9.8
115.1		2120	2198	2322	3.7	9.5
115.3	2800	2798	2975	3038	6.3	8.6
116.3	–	671	730	783	8.7	16.6
116.7	1095	1356	1408	1456	3.8	7.4
117.5	–	1245	1293	1309	3.8	5.1
117.7	1257	1950	2133	2235	9.4	14.6
119.0	–	1057	1110	1161	5.1	9.8
119.3	1113	1566	1728	1846	10.3	17.9
122.1	–	1878	2036	2186	8.4	16.4
122.4	2658	3886	4525	4890	16.4	25.8
125.9	2727	3104	3266	3364	5.2	8.4
129.2	5053	5361	5635	5769	5.1	7.6
131.6	–	661	684	727	3.5	10
132.9	–	860	879	930	2.3	8.1
136.5	2109	2042	2056	2108	0.7	3.2
141.1	4857	4738	4845	4872	2.3	2.8
145.0	6055	6125	6334	6315	3.4	3.1
150.4	1386	1452	1442	1437	−0.7	−1
154.6	307	242	200	202	−17.5	−16.8
155.9	–	240	212	198	−11.5	−17.2
159.8	–	209	164	123	−21.7	−41.3
161.0	236	217	186	142	−14.1	−34.3
162.9	–	135	94	61	−30.5	−55

and most diffuse bands: only 1% difference at 145 nm and 6% at 129.2 nm. On the contrary, large differences arise when comparing sharper peaks, for instance at 122.4 and 117.7 nm where we find peak intensities 50% higher than Connors et al.'s (see Table 1). The observed differences in the intensities of the sharpest peaks can be explained by the different spectral resolution used in both studies. The resolution is not given explicitly by Connors et al. (1974), but our HC_3N spectrum is clearly better resolved since it shows more detailed structure. For example, several new peaks can be distinguished at 119, 122.1 nm and between 114.4 and 118.2 nm.

Our mid-UV range measurements can be compared with those of Bénilan et al. (1994) in Table 2. Discrepancies of up to about 20% appear at room temperature and even more for some features at lower temperature. This clearly shows that our setup is much less precise in the mid-UV compared to the VUV, mainly due to the fluctuations of the synchrotron radiation above 200 nm and the small size of our cell as evoked earlier. In their study, Bénilan and colleagues used a deuterium lamp as light source and a 3 m long cell, specially adapted for the mid-UV domain.

3.1.2. Temperature dependence of the absorption coefficient of HC_3N between 170 and 225 nm

Fig. 3 shows the absolute absorption coefficient of HC_3N between 170 and 225 nm at the resolution of 0.05 nm

at three different temperatures: 298, 243 and 203 K. Our measurements confirm the temperature dependency highlighted by Bénilan et al. (1994, 1996). In particular, we observe an increase of the most intense bands and a decrease of the width of the bands when the temperature decreases. Temperature effects can be quantified by calculating the fractional change in cross-section value $P_{c,T}$. The change of cross-section values σ_T as a function of temperature T may be defined as the percent change $P_{c,T}$ which can be given as

$$P_{c,T} = 100 \times \frac{\sigma_T - \sigma_{298}}{\sigma_{298}} \quad (2)$$

A negative or a positive $P_{c,T}$ value means that the absorption coefficient at a temperature T is respectively smaller or larger than that at 298 K.

The absolute absorption coefficients versus temperature at different peak positions is shown in Table 2, together with the percentage change $P_{c,T}$. The absorption coefficient for the intense absorption peak at 224.7 nm increases by 31% from 40.9 to 53.6 $\text{cm}^{-1} \text{am}^{-1}$ when the temperature decreases from 298 to 203 K. A similar increase, between 20% and 34%, is observed for the other three main peaks at 196.9, 205.2 and 214.6 nm. Our $P_{c,T}$ values are very close to those obtained by Bénilan and colleagues (see Table 2).

Table 2

Mid-UV absorption coefficients (in $\text{cm}^{-1} \text{am}^{-1}$) of cyanoacetylene for various features measured at selected temperatures in this work and in previous work (Bénilan et al., 1994) with the percentage changes $P_{c, 203 \text{ K}}$ and $P_{c, 243 \text{ K}}$.

λ (nm)	Bénilan et al. (1994) at 293 K	Bénilan et al. (1994) at 213 K	σ (298 K)	σ (243 K)	σ (203 K)	$P_{c, 243 \text{ K}}$	$P_{c, 203 \text{ K}}$
189.2	–	–	10.2	8.9	11.7	–12.8	15.3
193.4	9.0	8.3	9.7	9.3	11.5	–3.7	18.7
195.2	11.8	16.8	11.0	11.6	14.5	5.7	31.5
196.4	10.5	10.0	10.2	10.3	12.1	1	18
196.9	19.8	20.5	19.7	22.0	25.9	11.8	31.4
200.8	7.4	6.9	6.9	6.4	10.0	–7.8	43.6
201.4	9.9	10.5	10.2	11.1	14.4	9	41.1
203.3	13.5	15.5	14.5	15.2	19.6	4.7	35.3
204.8	14.8	19.0	16.4	18.3	22.5	12	37.7
205.2	28.4	38.5	34.3	37.5	45.9	9.5	34
210.3	9.4	8.9	10.2	9.3	10.5	–9	2.3
212.1	14.1	16.5	14.6	16.2	18.2	10.8	24.3
212.5	12.0	13.3	12.9	13.1	14.9	1.9	16.3
214.0	19.7	26.8	23.5	25.4	31.0	8	32
214.2	24.3	31.8	24.6	28.1	33.4	14.3	35.9
214.2	21.4	25.8	23.7	24.1	28.4	1.8	19.9
214.6	37.9	48.3	45.8	49.2	55.0	7.4	19.9
221.9	7.8	9.8	8.6	11.2	12.8	30.2	49.1
222.4	8.4	10.8	8.8	11.8	13.3	34.7	51.7
224.1	14.0	20.1	16.2	19.2	20.0	18.3	23
224.2	17.1	22.9	19.5	21.5	22.2	10.5	14.1
224.7	33.7	47.6	40.9	47.6	53.6	16.5	31

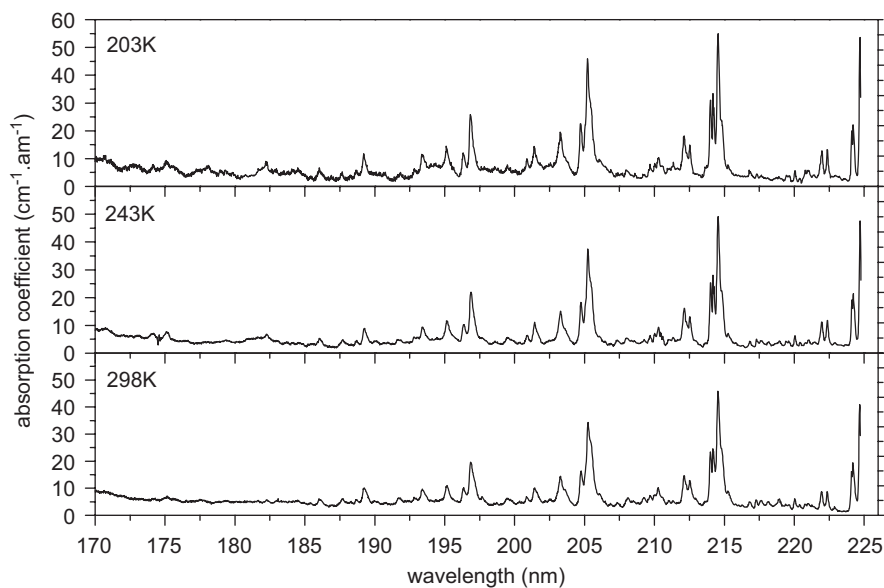


Fig. 3. Absolute absorption coefficient of HC_3N between 170 and 225 nm measured at 203, 243 and 298 K.

3.1.3. Temperature dependence of the absorption coefficient of HC_3N between 115 and 170 nm

The photoabsorption cross-section of HC_3N at low temperature has been measured for the first time in the VUV region. As seen in Fig. 4, the spectra obtained at different temperatures are not significantly different. The absorption coefficients of the main bands at 298, 243 and 203 K are listed in Table 1, together with the $P_{c,T}$ values.

For the large and diffuse bands at 125.9, 129.2, 141.1 and 145 nm, the variation of the peak absorption coefficient is $<10\%$ in the studied temperature range. This is within the quoted experimental error. Only the sharpest absorption features show significant temperature effects. For example, the band at 122.4 nm shows an increase from 3886 to 4890 $\text{cm}^{-1} \text{am}^{-1}$ for a temperature change from 298 to 203 K. This variation can be explained by a rearrangement

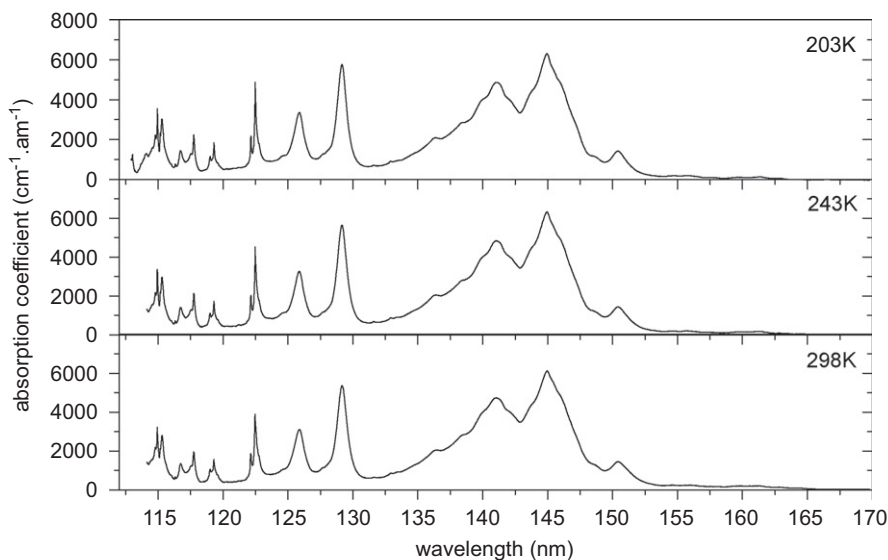


Fig. 4. Absolute absorption coefficient of HC_3N between 112 and 170 nm measured at 203, 243 and 298 K.

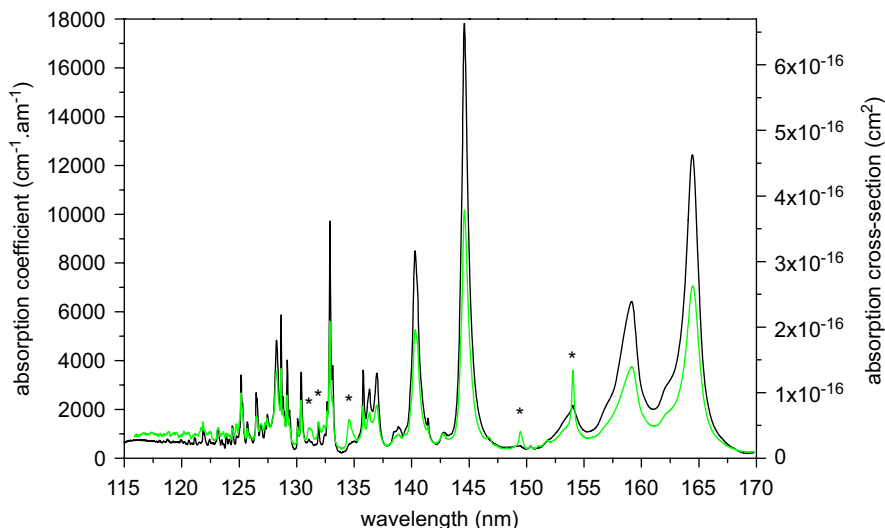


Fig. 5. The absorption spectrum of C_4H_2 between 115 and 170 nm at 268 K obtained with a pure sample (black line) compared to the one at room temperature (green line). The comparison shows the C_4H_2 sample at 293 K contains an impurity, its the main features being identified by stars.

of the rovibrational population distribution that favours sharper band profiles when the gas temperature is reduced. Since the transition moment must be conserved, larger cross-sections peaks are usually observed at low temperatures. The broadening of the bands, caused by the predissociation of the molecule, prevents observation of this phenomenon in the large and diffuse bands. This explains qualitatively the greater variations observed for the sharper peaks as compared to the broad ones. It also explains the minor role of the temperature in the 112–170 nm domain, compared to the mid-UV where predissociation is less strong. We also observe large negative $P_{c,T}$ values between 152 and 164 nm. This is very likely an indication that the absorption originates from an excited vibrational level of the ground electronic state.

3.2. Diacetylene

3.2.1. Preliminary remarks on the purity of the sample

In spite of all precautions that were taken during the synthesis of C_4H_2 (including IR spectral control of the sample) the presence of an impurity has been revealed in spectra between 115 and 170 nm. The impurity is possibly 2-chloro-1-butene-3-yne ($\text{C}_4\text{H}_3\text{Cl}$), a compound that could have formed by the elimination of only one equivalent HCl from the compound 1,4-dichloro-2-butyne ($\text{C}_4\text{H}_4\text{Cl}_2$) (Khlifi et al., 1995). It has been observed by several other groups (Georgieff and Richard, 1958; Smith et al., 1998). The contamination is identified by one peak at 154.3 nm and several other smaller features (134.8, 149.7 and 131–133 nm) which vary in intensity due to the evolving composition of our sample. In fact, outgassing enhanced the

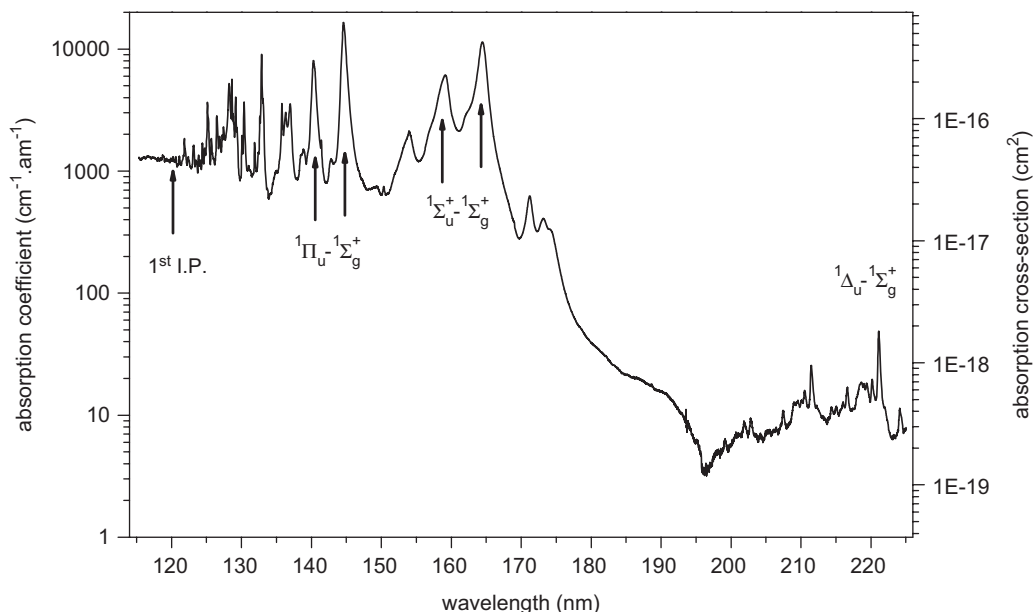


Fig. 6. The photoabsorption cross-section of C_4H_2 on a logarithmic scale in the 115–225 nm at ambient temperature (293 K). The main electronic transitions are shown.

purity of our sample during the measurements. Finally, our last spectrum, obtained at 268 K, does not show any impurity absorption peaks unlike the spectrum obtained at 293 K, as seen in Fig. 5. By considering the latter as free of impurity, the spectrum of the impurity could be estimated by subtraction and the partial pressure of the impurity contained in each sample can be calculated. Assuming that the impurity spectrum does not vary with temperature, the pressure corrections that have been applied to obtain the C_4H_2 absorption coefficients are 15% at 298 and 243 K, 5% at 203 K and 20% at 173 K.

3.2.2. Photoabsorption by C_4H_2 at 293 K

The absorption coefficient of C_4H_2 measured at 293 K and 0.05 nm resolution in the 115–225 nm range is shown in Fig. 6, together with the cross-section values.

As it is the case for HC_3N , the absorption spectrum of C_4H_2 can be clearly divided into two parts. The first one, between 195 and 225 nm, shows structured vibrational progressions which were assigned to a ${}^1\Delta_u \leftarrow {}^1\Sigma_g^+$ forbidden electronic transition by Haink and Jungen (1979). The second region, between 115 and 175 nm, shows a succession of several strong absorption features. The spectrum consists mainly of two allowed electronic transitions with vibrational progressions. An intense and diffuse band, assigned to the origin of the ${}^1\Sigma_u \leftarrow {}^1\Sigma_g^+$ transition, is observed at 164.4 nm (Smith, 1967). Two peaks at 159.1 and 154 nm corresponding to a vibrational progression with spacings of about 2000 cm^{-1} are assigned to the excitation of the ν_2 vibrational $C\equiv C$ stretching. The prominent peak at 144.6 nm is assigned to the origin of the ${}^1\Pi_u \leftarrow {}^1\Sigma_g^+$ transition (Smith, 1967). This transition also shows a vibrational progression with peaks at 140.3 and

Table 3

Relative absorption coefficients at low temperatures of diacetylene for the two main peaks in mid-UV, in this work and in previous works.

λ (nm)	$\sigma_{223}/\sigma_{295\text{ K}}$ Fahr and Nayak (1994)	$\sigma_{193}/\sigma_{293\text{ K}}$ Smith (1967)	$\sigma_{203}/\sigma_{293\text{ K}}$ from this work
211.3	1.03	1.31	1.16
221	1.05	1.38	1.33

136.4 nm. Almost all the strong peaks belong to the R and R' Rydberg series leading both to the first ionization energy at 10.18 eV (121.9 nm). At shorter wavelength a third Rydberg R'' series, with associated ν_2 vibration progressions, was identified by Smith (1967).

3.2.3. Temperature dependence of the absorption coefficient of C_4H_2 between 195 and 225 nm

The absorption coefficient of C_4H_2 has been measured from 180 to 225 nm at two temperatures, 293 and 203 K. As shown in Table 3, we measure a significant temperature effect for the strongest peaks at 211.3 and 221 nm. In order to compare this temperature dependence with that observed with previous studies by Fahr and Nayak (1994) and Smith et al. (1998), we list in Table 3 the ratio between low- and room-temperature cross-sections. Fahr and Nayak saw almost no change from 295 to 223 K, but according to Smith et al. (1998), the presence of an impurity (C_4H_3Cl) biased their study of the temperature dependence. On the contrary, the results of these authors (Smith et al., 1998) are comparable to ours, considering experimental errors (see Table 3).

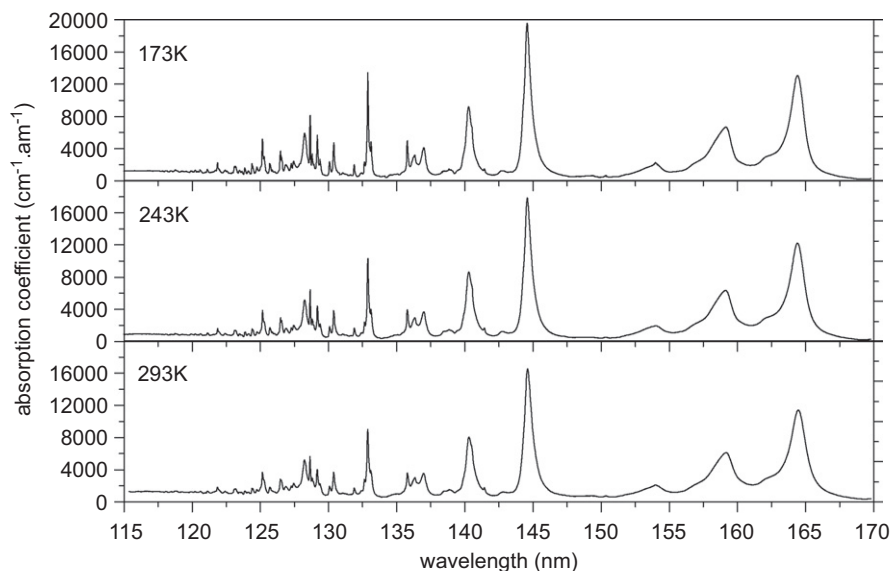


Fig. 7. Absorption coefficient of C_4H_2 between 115 and 170 nm at different temperatures: 293, 243 and 173 K.

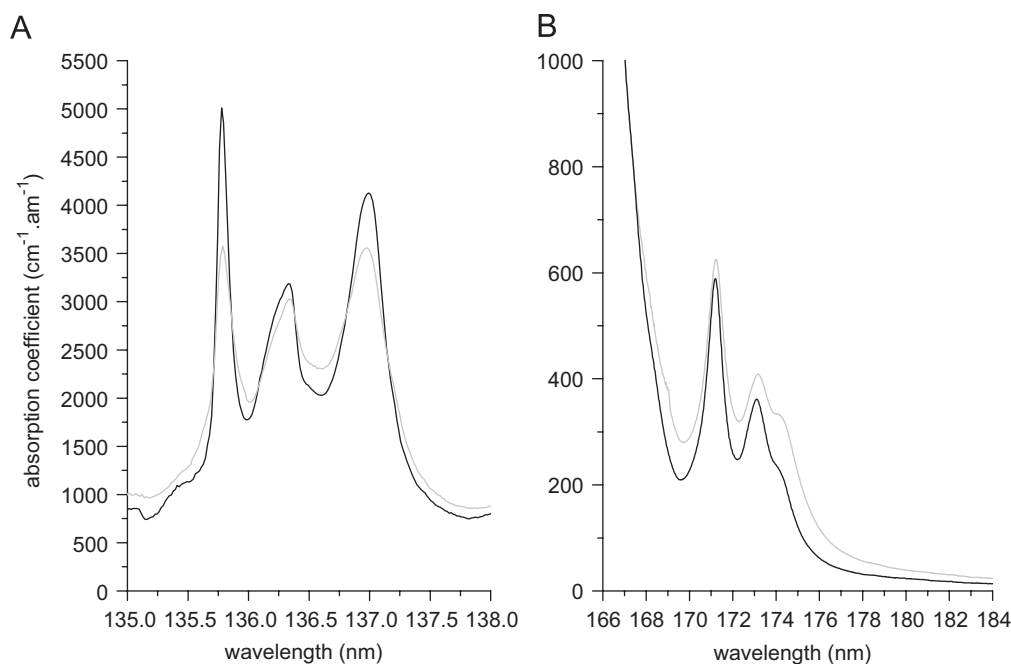


Fig. 8. Variation in the structure of the absorption coefficient of C_4H_2 in the regions 135–138 nm (panel A) and 166–184 nm (panel B) against temperature for 293 K (gray line) and 173 K (dark line).

3.2.4. Temperature dependence of the absorption coefficient of C_4H_2 between 115 and 170 nm

Here, we present the first VUV low temperatures absorption coefficients for C_4H_2 in the 115–170 nm wavelength range (268, 243, 203 and 173 K). The corresponding spectra are presented in Fig. 7 for 173, 243 and 293 K. Most of the peaks show an intensity enhancement at low temperature compared to room temperature. The sharpest feature at 132.9 nm shows the strongest variation. It increases by 50% when the temperature decreases from room temperature to 173 K. Narrowing of the band width

is also clearly observed for this band. In Fig. 8, we show an example of the influence of the temperature on the line shape of three overlapping transitions between 135 and 138 nm (Fig. 8A) and in the 166–184 nm interval (Fig. 8B). In the 135–138 nm interval, as the temperature decreases, the background continuum decreases and the band profile becomes narrower. Furthermore, the maxima of the three band increase. This effect is due to the redistribution of the population towards lower rotational energy levels with decreasing temperature. This is expected in the case of cold bands originating from the vibrational ground state. In the

Table 4

Absorption cross-section (in $\text{cm}^{-1} \text{am}^{-1}$) of C_4H_2 for selected peaks at different temperatures and comparison with the work of Okabe (1981).

λ (nm)	σ_{293}	Okabe (1981)	$\sigma_{293}/\sigma_{\text{Okabe}}$	σ_{268}	σ_{243}	σ_{203}	σ_{173}
125.2	3661	2767	1.3	3416	3892	4229	5179
128.7	5655	3573	1.6	5873	6429	7036	8116
129.2	4034	2260	1.8	4027	4425	4850	5694
130.4	3692	2010	1.8	3531	3852	4078	4737
132.9	9022	2767	3.3	9723	10 317	11 617	13 464
135.8	3580	2139	1.7	3616	3961	4350	5009
137.0	3556	ind.	–	3487	3687	3783	4127
140.3	8284	5964	1.4	8495	8655	9053	9572
144.6	16 548	6153	2.7	17 820	17 829	18 956	19 560
159.1	6117	4621	1.3	6428	6365	6680	6691
164.4	11 418	5695	2	12,435	12 226	13 135	13 082

region 166–184 nm, we also observe a decrease of the background continuum as the temperature decreases. The band maxima decrease, however. This effect is certainly due to the combination of the redistribution over rotational levels for the cold bands and the presence of hot bands originating from excited vibrational levels (Table 4).

The absorption coefficient of C_4H_2 has been measured by Okabe (1981) and by Fahr and Nayak (1994). Okabe has measured the absorption cross-sections between 120 and 180 nm at 0.08 nm resolution and room temperature. Our values are approximately a factor of two higher than those determined by Okabe, for the most intense bands. Our absorption coefficient at 132.9 nm is even three times higher than the value reported by Okabe. These discrepancies are mainly due to saturation problems in Okabe's study as already mentioned by Shemansky et al. (2005) and Jolly and Bénilan (2008). Indeed, Okabe has used an absorption cell ten times longer than ours and a minimum pressure of 60 μbars which leads to zero transmission for the most intense bands. Fahr and Nayak (1994) have measured the absorption cross-section between 160 and 260 nm at a resolution of 0.2 nm, as well as the temperature dependence between 220 and 300 K. They took great care of avoiding saturation and showed a significant temperature dependence of the absorption cross-section. Our results at room temperature show a good agreement between 160 and 175 nm: our values are slightly lower, by 5% for the 164.4 nm and larger, by 15%, for the weak band at 171 and 173 nm. These differences are possibly due to a better resolution in the present study.

Temperature effects are presented in Fig. 9 where the percentage changes $P_{c,T}$ are presented for various peaks at four different temperatures. Except for the two sharpest features (132.9 and 129.7 nm) where the relative variation reaches 50%, we observe effects of 8–18% for the most intense bands when the temperature decreases from 293 to 173 K. For the band at 164.4 nm, which is the only one for which we can make a comparison with the results of Fahr and Nayak (1994), we find a 15% increase when lowering the temperature from 300 to 203 K whereas they found a

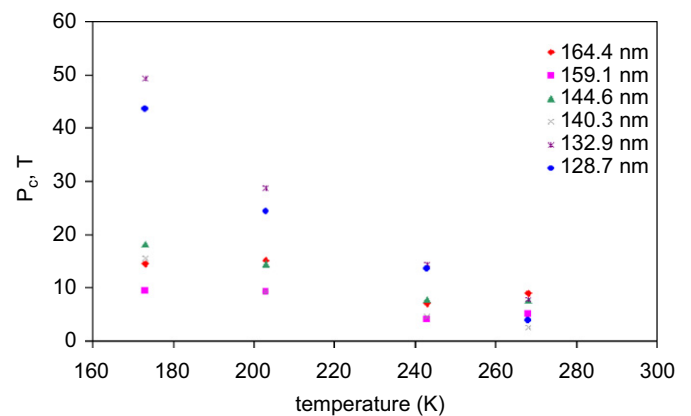


Fig. 9. The percentage change $P_{c,T}$ for C_4H_2 for different temperatures and for selected wavelengths.

30% increase for the absorption coefficient measured at 223 K. Fahr and Nayak do not give experimental errors, however their results are reproducible within 2%. Thus, there seems to be a significant difference compared to our measurements. This remains to be clarified in the future.

4. Implications for the interpretation of Titan's atmospheric spectra

From observations of a stellar occultation, the Cassini UVIS experiment (Esposito et al., 2004) was able to measure transmission spectra of Titan's atmosphere in the far ultraviolet (Shemansky et al., 2005). Absorption cross-sections at low temperatures are necessary to interpret satisfactorily these observations which sound the upper atmosphere of Titan. By analysing the atmospheric transmission spectra, Shemansky et al. (2005) were able to infer the vertical distribution of the absorbing species. Whereas HC_3N was not detected, in the case of C_4H_2 , difficulties appeared in the analysis due to Okabe's erroneous absorption cross-section data, as concluded by Shemansky et al. (2005)

In order to test the influence on the analysis of UVIS data of our new absorption cross-sections obtained at low

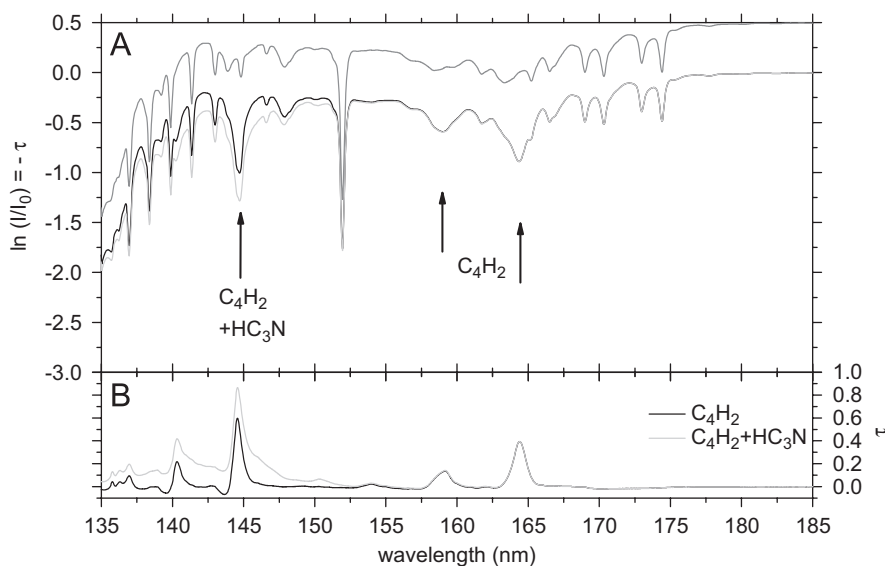


Fig. 10. Expected Titan's transmission spectra simulated in the 135–185 nm range (in panel A). The first one (gray line shifted upward by 0.5 for clarity) is obtained using the last available absorption spectra for CH_4 , C_2H_2 , C_2H_4 , C_2H_6 and HCN with the following column densities (cm^{-2}): $\text{CH}_4 = 1.9 \times 10^{17}$, $\text{C}_2\text{H}_2 = 1.1 \times 10^{16}$, $\text{C}_2\text{H}_4 = 8.2 \times 10^{15}$, $\text{C}_2\text{H}_6 = 7.3 \times 10^{15}$, $\text{HCN} = 1.9 \times 10^{16}$. A second simulation (black line) integrates absorption from C_4H_2 reported in this present work with an abundance value of $1.3 \times 10^{15} \text{cm}^{-2}$. The transmission spectrum in light gray line incorporates absorption from HC_3N with the same abundance value as the one of C_4H_2 . Panel B shows the optical densities corresponding to the last two cases.

temperatures for C_4H_2 and HC_3N , we have simulated transmission spectra to be expected at high altitude in Titan's atmosphere (cf. Fig. 10).

Considering the available absorption cross-sections for the main molecular species, CH_4 , C_2H_6 (Chen and Wu, 2004), C_2H_2 (Wu et al., 2001), C_2H_4 (Wu et al., 2004) and HCN (Nuth and Glicker, 1982), the expected transmission spectra can be calculated using the column densities values given by Shemansky et al. (2005) in Fig. 2 of their paper. The calculated transmission spectrum is then convoluted by a boxcar function with a width of 0.275 nm to match UVIS resolution. It is shown as a gray line in Fig. 10A.

We obtain a second transmission spectrum (black line in Fig. 10A) by adding our absorption cross-section of C_4H_2 and taking an abundance value of $1.3 \times 10^{15} \text{cm}^{-2}$ as proposed by Shemansky et al. (2005). As seen in Fig. 10, strong C_4H_2 absorption features appear at 144.6 and 164.4 nm due to C_4H_2 . These features are clearly observed in the UVIS transmission spectra of Titan's atmosphere as can be seen in Fig. 2 of Shemansky's paper, but they were lacking in their model which uses Okabe's saturated absorption data for C_4H_2 . Our measured absorption cross-sections for C_4H_2 should significantly improve the analysis of the transmission spectra and the determination of its column densities at different altitudes and latitudes. Since absorption maxima in the main bands are enhanced as compared to previous reference data and since they increase with decreasing temperature, we can expect a lower abundance of C_4H_2 than the proposed value by Shemansky et al. (2005).

A third simulation (light gray line) is done by adding our HC_3N absorption cross-sections at the same abundance like C_4H_2 ($1.3 \times 10^{15} \text{cm}^{-2}$) because recent results from

photochemical models (Hébrard et al., 2007) predict that these two compounds are present in Titan's atmosphere at approximately the same concentration. Unlike in the low-resolution Voyager observations (Vervack et al., 2004), the contribution of the two species HC_3N and HCN in the region 135–150 nm, can be well separated with UVIS which have a resolving power ten times higher. However, it is now the similarity of the spectral features of HC_3N and C_4H_2 which makes them difficult to separate. Nevertheless, as can be seen in Fig. 10B, the optical depth at 144.6 nm increases when HC_3N is present. This leads to a change in the relative intensity of the two main absorption bands of C_4H_2 at 145 and 165 nm. These effects should be easily visible in the observed transmission spectra taken by UVIS if the signal to noise ratio is good enough. This could lead to the first UV detection and quantification of HC_3N in the upper atmosphere of Titan.

5. Conclusion

We have determined the absorption coefficients for two gaseous organic species, HC_3N and C_4H_2 , from the vacuum UV spectral region up to the mid UV. The absorption cross-sections were determined at 0.05 nm resolution in the 80–225 nm range for HC_3N , and between 115 and 225 nm for C_4H_2 . The resolution that we have used has allowed us to observe several sharp features which had not been observed before. Special care has been taken to ensure that the absorption coefficients were not obtained from saturated spectra. Thus, in the case of C_4H_2 , significantly higher absorption coefficients were obtained as compared to the previously reported values by Okabe (1981). To a lesser extent, absorption coefficients measured

for HC_3N are also generally larger than the values of Connors et al. (1974).

The study in the 180–225 nm region has confirmed the temperature dependence of the absorption coefficient reported by earlier studies. No significant temperature dependencies for the cross-sections in the 112–170 nm domain over the 203–298 K temperature range have been observed for HC_3N . However, in the same wavelength range, the absorption coefficient of C_4H_2 clearly increases by 50% for sharp peaks when the temperature is changed from 296 to 173 K. Under low-temperature conditions, we note an almost linear increase of both the absorption maxima and the narrowing of the band profile. This is interpreted in terms of the change of the population of the rovibrational levels. Since the mid-UV and VUV measurements were obtained in the same experimental conditions, and since the results in the mid-UV agree with previous studies, it confirms that in the VUV the temperature effects are important in the case of C_4H_2 but not for HC_3N . The absorption bands of C_4H_2 are much narrower than those of HC_3N in the same wavelength range explaining the different behavior observed for these compounds.

These new results will improve the interpretation of Titan transmission spectra. Detection of HC_3N by UVIS and a more accurate determination of the vertical profile of C_4H_2 are expected.

More data at low temperature would be needed to improve the modeled transmission of limb spectra obtained by UVIS. For example, the model still uses room temperature cross-sections for HCN. The determination of HCN cross-sections at low temperature is clearly needed.

All the spectra presented here can be found in our spectroscopic data base at the following internet link: <http://www.lisa.univ-paris12.fr/GPCOS/SCOOPweb/SCOOP.html>.

Acknowledgements

The authors wish to thank Dr. Gerd Reichardt for his excellent assistance during the synchrotron radiation beam time periods. We acknowledge the financial support of the European Commission Programme “Access to Research Infrastructures” in providing access to the synchrotron BESSY at Berlin. We also acknowledge the financial support of the French CNRS program PNP.

References

- Andrieux, D., Bénilan, Y., de Vanssay, E., Paillous, P., Khlifi, M., Raulin, F., Bruston, P., Guillemin, J.-C., 1995. Absorption coefficient of propynenitrile in the mid-UV range for the study of Titan's atmosphere: solution to sample contaminations. *J. Geophys. Res.* 100, 9455–9460.
- Bell, M.B., Feldman, P.A., Travers, M.J., McCarthy, M.C., Gottlieb, C.A., Thaddeus, P., 1997. Detection of HC_{11}N in the cold dust cloud TMC-1. *Astrophys. J.* 483, L61.
- Bénilan, Y., Bruston, P., Raulin, F., Cossart-Magos, C., Guillemin, J.-C., 1994. Mid-UV spectroscopy of propynenitrile at low temperature: consequences on expected results from observations of Titan's atmosphere. *J. Geophys. Res.* 99, 17069–17074.
- Bénilan, Y., Andrieux, D., Khlifi, M., Bruston, P., Raulin, F., Guillemin, J.-C., Cossart-Magos, C., 1996. Temperature dependence of HC_3N , C_6H_2 , and C_4N_2 mid-UV absorption coefficients. Application to the interpretation of Titan's atmospheric spectra. *Astrophys. Space Sci.* 236, 85–95.
- Bruston, P., Poncet, H., Raulin, F., Cossart-Magos, C., Courtin, R., 1989. UV spectroscopy of Titan's atmosphere, planetary organic chemistry, and prebiological synthesis: I. Absorption spectra of gaseous propynenitrile and 2-butyne nitrile in the 185- to 250-nm region. *Icarus* 78, 38–53.
- Cernicharo, J., Heras, A.M., Tielens, A.G.G.M.P., Pardo, J.R., Herpin, F., Guélin, M., Waters, L.B.F.M., 2001. Infrared space observatory's discovery of C_4H_2 , C_6H_2 , and Benzene in CRL 618. *Astrophys. J.* 546, L123–L126.
- Chen, F.Z., Wu, C.Y.R., 2004. Temperature-dependent photoabsorption cross sections in the VUV-UV region. I. Methane and ethane. *J. Quant. Spectrosc. Radiat. Transfer* 85, 195–209.
- Connors, R.E., Roebber, J.L., Weiss, K., 1974. Vacuum ultraviolet spectroscopy of cyanogen and cyanoacetylenes. *J. Chem. Phys.* 60, 5011–5024.
- Coustenis, A., Bézard, B., 1995. Titan's atmosphere from voyager infrared observations: IV. Latitudinal variations of temperature and composition. *Icarus* 115, 126–140.
- Coustenis, A., Salama, A., Schulz, B., Ott, S., Lellouch, E., Encrenaz, T., Gautier, D., Feuchtgruber, H., 2003. Titan's atmosphere from ISO mid-infrared spectroscopy. *Icarus* 161, 383–403.
- Coustenis, A., Achterberg, R.K., Conrath, B.J., Jennings, D.E., Marten, A., Gautier, D., Nixon, C.A., Flasar, F.M., Teanby, N.A., Bézard, B., Samuelson, R.E., Carlson, R.C., Lellouch, E., Bjoraker, G.L., Romani, P.N., Taylor, F.W., Irwin, P.G.J., Fouchet, T., Hubert, A., Orton, G.S., Kunde, V.G., Vinatier, S., Mondellini, J., Abbas, M.M., Courtin, R., 2007. The composition of Titan's stratosphere from Cassini/CIRS mid-infrared spectra. *Icarus* 189, 35–62.
- Esposito, L.W., Barth, C.A., Colwell, J.E., Lawrence, G.M., McClintock, W.E., Stewart, A.I.F., Keller, H.U., Korth, A., Lauche, H., Festou, M.C., Lane, A.L., Hansen, C.J., Maki, J.N., West, R.A., Jahn, H., Reulke, R., Warlich, K., Shemansky, D.E., Yung, Y.L., 2004. The Cassini ultraviolet imaging spectrograph investigation. *Space Sci. Rev.* 115, 299–361.
- Fahr, A., Nayak, A.K., 1994. Temperature dependent ultraviolet absorption cross sections of 1,3-butadiene and butadiyne. *Chem. Phys.* 189, 725–731.
- Flasar, F.M., Achterberg, R.K., Conrath, B.J., Gierasch, P.J., Kunde, V.G., Nixon, C.A., Bjoraker, G.L., Jennings, D.E., Romani, P.N., Simon-Miller, A.A., Bézard, B., Coustenis, A., Irwin, P.G.J., Teanby, N.A., Brasunas, J., Pearl, J.C., Segura, M.E., Carlson, R.C., Mamoutkine, A., Schinder, P.J., Barucci, A., Courtin, R., Fouchet, T., Gautier, D., Lellouch, E., Marten, A., Prangé, R., Vinatier, S., Strobel, D.F., Calcutt, S.B., Read, P.L., Taylor, F.W., Bowles, N., Samuelson, R.E., Orton, G.S., Spilker, L.J., Owen, T.C., Spencer, J.R., Showalter, M.R., Ferrari, C., Abbas, M.M., Raulin, F., Edgington, S., Ade, P., Wishnow, E.H., 2005. Titan's atmospheric temperatures, winds, and composition. *Science* 308, 975–978.
- Georgieff, K.K., Richard, Y., 1958. Diacetylene: preparation, purification, and ultraviolet spectrum. *Can. J. Chem.* 36, 1280–1283.
- Glicker, S., Okabe, H., 1987. Photochemistry of diacetylene. *J. Phys. Chem.* 91, 437–440.
- Haink, H.-J., Jungen, M., 1979. Excited states of the polyacetylenes. Analysis of the near ultraviolet spectra of diacetylene and triacetylene. *Chem. Phys. Lett.* 61, 319–322.
- Hanel, R., Conrath, B., Flasar, F.M., Kunde, V., Maguire, W., Pearl, J.C., Pirraglia, J., Samuelson, R., Herath, L., Allison, M., Cruikshank, D.P., Gautier, D., Gierasch, P.J., Horn, L., Koppany, R., Ponnampereuma, C., 1981. Infrared observations of the Saturnian system from voyager 1. *Science* 212, 192–200.

- Hébrard, E., Dobrijevic, M., Bénilan, Y., Raulin, F., 2007. Photochemical kinetics uncertainties in modeling Titan's atmosphere: first consequences. *Planet. Space Sci.* 55, 1470–1489.
- Hunter, W.R., Malo, S.A., 1969. The temperature dependence of the short wavelength transmittance limit of vacuum ultraviolet window materials—I. Experiment. *J. Phys. Chem. Solids* 30, 2739–2745.
- Job, V.A., King, G.W., 1966. The electronic spectrum of cyanoacetylene: part II. Analysis of the 2300-Å system. *J. Mol. Spectrosc.* 19, 178–184.
- Jolly, A., Bénilan, Y., 2008. Review of quantitative spectroscopy of polyynes. *J. Quant. Spectrosc. Radiat. Transfer* 109, 963–973.
- Jolly, A., Bénilan, Y., Fayt, A., 2007. New infrared integrated band intensities for HC₃N and extensive line list for the *n*₅ and *n*₆ bending modes. *J. Mol. Spectrosc.* 242, 46–54.
- Khlifi, M., Paillous, P., Delpech, C., Nishio, M., Bruston, P., Raulin, F., 1995. Absolute IR band intensities of diacetylene in the 250–4300 cm⁻¹ region: implications for Titan's atmosphere. *J. Mol. Spectrosc.* 174, 116–122.
- Kloster-Jensen, E., Haink, H.-J., Christen, H., 1974. The electronic spectra of unsubstituted Mono- to pentaacetylene in the gas phase and in solution in the range 1100–4000 Å. *Helv. Chim. Acta* 57, 1731–1744.
- Kunde, V.G., Aikin, A.C., Hanel, R.A., Jennings, D.E., Maguire, W.C., Samuelson, R.E., 1981. C₄H₂, HC₃N and C₂N₂ in Titan's atmosphere. *Nature* 292, 686–688.
- Lavvas, P.P., Coustenis, A., Vardavas, I.M., 2008. Coupling photochemistry with haze formation in Titan's atmosphere, part I: model description. *Planet. Space Sci.* 56, 27–66.
- Miller, F.A., Lemmon, D.H., 1967. The infrared and Raman spectra of dicyanodiacetylene. *Spectrochim. Acta* 23A, 1415–1423.
- Moureu, C., Bongrand, J.C., 1920. Le cyanoacetylene C₃NH. *Ann. Chim.* 14, 47.
- Niemann, H.B., Atreya, S.K., S.J. Bauer, G.R.C., Demick, J.E., Frost, R.L., Gautier, D., Haberman, J.A., Harpold, D.N., Hunten, D.M., Israel, G., Lunine, J.I., Kasprzak, W.T., Owen, T.C., Paulkovich, M., Raulin, F., Raaen, E., Way, S.H., 2005. The abundances of constituents of Titan's atmosphere from the GCMS instrument on the Huygens probe. *Nature* 438, 779–784.
- Nuth, J.A., Glicker, S., 1982. The vacuum ultraviolet spectra of HCN, C₂N₂ and CH₃CN. *J. Quant. Spectrosc. Radiat. Transfer* 28, 223–231.
- Okabe, H., 1981. Photochemistry of acetylene at 1470 Å. *J. Photochem.* 17, 172–184.
- Orgel, L.E., 2002. Is cyanoacetylene prebiotic? *Origins Life Evol. Biosphere* 32, 279–281.
- Reichardt, G., Bahrtdt, J., Schmidt, J.-S., Gudat, W., Ehresmann, A., Müller-Albrecht, R., Molter, H., Schmoranzner, H., Martins, M., Schwentner, N., Sasaki, S., 2001a. A 10 m-normal incidence monochromator at the quasi-periodic undulator U125-2 at BESSY II. *Nucl. Instrum. Methods Phys. Res., Sect. A* 467–468, 462–465.
- Reichardt, G., Noll, T., Packe, I., Rotter, P., Schmidt, J.-S., Gudat, W., 2001b. Adaption of the BESSY I-3 m normal incidence monochromators to the BESSY II source. *Nucl. Instrum. Methods Phys. Res. Sect. A* 467–468, 458–461.
- Shemansky, D.E., Stewart, A.I.F., West, R.A., Esposito, L.W., Hallett, J.T., Liu, X., 2005. The Cassini UVIS stellar probe of the Titan atmosphere. *Science* 308, 978–982.
- Smith, W.L., 1967. The absorption spectrum of diacetylene in the vacuum ultraviolet. In: *Proceedings of the Royal Society of London. Series A Mathematical and Physical Sciences*. Vol. 300, pp. 519–533.
- Smith, B.A., Soderblom, L., Beebe, R.F., Boyce, J.M., Briggs, G., Bunker, A., Collins, S.A., Hansen, C., Johnson, T.V., Mitchell, J.L., Terrile, R.J., Carr, M.H., Cook, A.F., Cuzzi, J.N., Pollack, J.B., Danielson, G.E., Ingersoll, A.P., Davies, M.E., Hunt, G.E., Masursky, H., Shoemaker, E.M., Morrison, D., Owen, T., Sagan, C., Veverka, J., Strom, R., Suomi, V.E., 1981. Encounter with Saturn—Voyager 1 imaging science results. *Science* 212, 163–191.
- Smith, N.S., Bénilan, Y., Bruston, P., 1998. The temperature dependent absorption cross sections of C₄H₂ at mid ultraviolet wavelengths. *Planet. Space Sci.* 46, 1215–1220.
- Teanby, N.A., Irwin, P.G.J., de Kok, R., Vinatier, S., Bézard, B., Nixon, C.A., Flasar, F.M., Calcutt, S.B., Bowles, N.E., Fletcher, L., Howett, C., Taylor, F.W., 2007. Vertical profiles of HCN, HC₃N, and C₂H₂ in Titan's atmosphere derived from Cassini/CIRS data. *Icarus* 186, 364–384.
- Turner, B.E., 1971. Detection of interstellar cyanoacetylene. *Astrophys. J.* 163, L35–L39.
- Vervack, R.J., Sandel, B.R., Strobel, D.F., 2004. New perspectives on Titan's upper atmosphere from a reanalysis of the voyager 1 UVS solar occultations. *Icarus* 170, 91–112.
- Waite, J.J., Niemann, H., Yelle, R.V., Kasprzak, W.T., Cravens, T.E., Luhmann, J.G., McNutt, R.L., Ip, W.H., Gell, D., De La Haye, V., Müller-Wordag, I., Magee, B., Borggren, N., Ledvina, S., Fletcher, G., Walter, E., Miller, R., Scherer, S., Thorpe, R., Xu, J., Block, B., Arnett, K., 2005. Ion neutral mass spectrometer results from the first flyby of Titan. *Science* 308, 90.
- Wu, C.Y.R., Chen, F.Z., Judge, D.L., 2001. Measurements of temperature-dependent of temperature cross sections of C₂H₂ in the VUV-UV region. *J. Geophys. Res.* 106, 7629–7636.
- Wu, C.Y.R., Chen, F.Z., Judge, D.L., 2004. Temperature-dependent photoabsorption cross sections in the VUV-UV region: Ethylene. *J. Geophys. Res.* 109, E07S15.
- Yung, Y.L., Allen, M., Pinto, J.P., 1984. Photochemistry of the atmosphere of Titan—comparison between model and observations. *Astrophys. J. Suppl. Ser.* 55, 465–506.